Integration of a Pulse Generator on Chip Into a Compact Ultrawideband Antenna

Alexander V. Vorobyov, *Member, IEEE*, Sumit Bagga, *Member, IEEE*, Alexander G. Yarovoy, *Senior Member, IEEE*, Sandro A. P. Haddad, *Member, IEEE*, Wouter A. Serdijn, *Member, IEEE*, John R. Long, *Member, IEEE*, Zoubir Irahhauten, *Member, IEEE*, and Leo P. Ligthart, *Fellow, IEEE*

***Abstract*—For impulse radio ultrawideband communications an "antenna plus generator" system is co-designed and an on chip generator is integrated into the antenna. This approach does away with the need for intermediate transmission lines conventionally placed between an RF device/generator and an antenna and therefore eliminates the need for a balun, prevents excitation of the common-mode currents and allows the device to be mounted directly on the antenna. The antenna and generator are designed taking into account both impedance matching and the generator's influence on the antenna's radiation properties. The suggested approach is verified experimentally at a scaled up version of the antenna.**

***Index Terms*—Antenna feed, antenna matching, balun, impulse radio (IR), integrated circuits, ultrawideband (UWB) antenna.**

I. Introduction

ANTENNAS for impulse radio ultrawideband (IR UWB) are considered to be one of the critical elements of the whole systems. The antenna should fulfill rigid specifications. Typical requirements are that they must radiate ultrashort pulses, that is, with a pulse width shorter than 1 ns, without considerable ringing, thus having an intrinsic operational bandwidth in excess of several gigahertz (i.e., ultimately from 3.1 to 10.6 GHz as allowed by the Federal FCC spectral mask [1]) and that the phase property of their transfer function should be linearly dependent on frequency. Moreover, UWB antennas must be well matched to the generator/transmitter or the receiver and have radiation efficiencies close to 100%. In order to be readily useable for many applications, the antenna should have omni-directional radiation patterns. Finally, an UWB antenna for mass market applications must be inexpensive to produce without this affecting its performance.

Among the many antenna designs recently proposed for impulse radio applications, [2]–[4] there are many variations of the classical bow-tie antenna, in which different flair profiles are used. One such antenna design is the "butterfly antenna"—so-called because of its elliptically-shaped flairs. This antenna is reported to be capable of radiating short pulses [5], [6] and to have a wide impedance bandwidth [7]. By fine-tuning the flair angle of this antenna with respect to the distance from the feeding point, one can obtain a flat input impedance over a large frequency band with a return loss of -15 dB or better, this being in the absence of sharp flair termination and thus leading to lower current reflections. Due to the large flair angle in the vicinity of the feeding point, the antenna has low input impedance and can be well matched to a 100 Ω feeding line. Despite its planar shape, the antenna also exhibits near-omnidirectional dipole-like patterns over a frequency span better than 3:1, making this antenna suitable for IR UWB applications.

The antenna also offers radiation efficiency greater than 90% within the operational band. Moreover, planar elliptical dipoles are electrically small and can be implemented on printed circuit board (PCB) substrates, which makes them inexpensive and readily feasible.

One drawback of the butterfly antenna is that it cannot easily be embedded into a device because it is centrally fed and has an input impedance larger than the typical generator output impedance (i.e., an impedance typically determined by that of the output transmission line); generally it is equal to 50 Ω. It is important to match the antenna well to the generator to increase radiated power and decrease ringing of the transmitted signal due to multiple reflections between the antenna and generator. However it is an extremely cumbersome task to design a compact, low-loss transient balun for feeding the antenna from an unbalanced line and matching the output impedance of the generator to the input impedance of the antenna. This was investigated in [8], [9]. To avoid use of balun in our previous paper [10] we investigated differential feeding of the antennas by a generator with differential outputs via a double semi-rigid cable, resulting in an improved match of the generator and the antenna, an improved magnitude response and reduced ringing of the radiated pulse. Presence of the transmission lines between the generator and antenna remains however a bottle-neck of the matching procedure and increases a total volume of the front-end.

In this paper, a procedure is proposed for tackling this issue: simply embed the generator directly on the antenna. Removing the conventional transmission lines (e.g., a microstrip, co-axial or semi-rigid cables) between the RF device and antenna allows for matching at any impedance value, giving extra flexibility for both antenna and RF designers. The co-design of the generator

Manuscript received July 19, 2006; revised September 10, 2007.

A. V. Vorobyov, A. G. Yarovoy, Z. Irahhauten, and L. P. Ligthart are with the International Research Center for Telecommunications and Radar, Faculty of Electrical Engineering, Mathematics and Computer Science (EEMCS), Delft University of Technology, 2628 CD, Delft, The Netherlands (e-mail: a.vorobyov@irctr.tudelft.nl; a.yarovoy@irctr.tudelft.nl).

S. Bagga, S. A. P. Haddad, W. A. Serdijn, and J. R. Long are with the Electronics research Laboratory, Faculty of Electrical Engineering, Mathematics and Computer Science (EEMCS), Delft University of Technology, 2628 CD, Delft, The Netherlands (e-mail: s.bagga@ewi.tudelft.nl; s.haddad@ewi.tudelft.nl; w.a.serdijn@ewi.tudelft.nl; j.r.long@ewi.tudelft.nl).

Digital Object Identifier 10.1109/TAP.2008.916900

and the antenna, both in terms of impedance matching and the influence of the former on radiation properties of the latter, leads to an optimum power transfer.

The co-design follows a three-step approach.

Step 1) Identify the interface between the RF device and the antenna (i.e., single-ended or differentially fed) and determine the shape of the waveform of the signal to be radiated;

Step 2) Perform an electromagnetic design synthesis (i.e., with the generator, antenna and PCB characteristics) to determine the antenna geometry, the position of the RF device with respect to the antenna flairs and the input impedance of the antenna;

Step 3) Design the output impedance of the generator accordingly.

We implemented the suggested above approach to demonstrate a principal possibility to embed RF chips directly in an UWB antenna. To reduce manufacturing costs and simplify technological implementation of RF chips we aimed at experimental realization of the co-design in the frequency band from 3 to 6 GHz.

Section II describes the electromagnetic model used for the co-design and the first step of the co-design related to the antenna feeding. The electromagnetic design of an "antenna plus generator" system is presented in Section III. RF circuit design is briefly discussed in Section IV, and finally, Section V gives the experimental verification and results.

II. Numerical Model

A commercial simulator like FEKO [11], which is based on the volumetric mixed-potential integral equation (MPIE) formulation, was used to develop a computational model of the "antenna plus generator". In the model, the antenna flairs, the feeding (i.e., strip) lines for the generator and the rectangular IC itself were assumed to be perfectly conducting and modeled by a surface current (see Fig. 1) under the assumption that the flairs and feeding lines are infinitely thin. The RF generator (in general, it can be any other RF device such as, e.g., LNA) occupies an area of about 1 mm^2. However, due to the external wiring and bias circuitry around the device, we estimated the total device area at about 2 mm^2. The generator is fed by two feeding lines (i.e., delivering the clock signal and a DC bias voltage), which are realized on the PCB as strip lines. All perfect electrically conducting (PEC) surfaces (including the chip) were subdivided into triangular surface elements. The Rao–Wilton–Glisson (RWG) basis functions were applied to these elements to obtain the equivalent electric and magnetic surface currents. The finite dielectric substrate of the PCB was subdivided into cuboids. Each element can be assigned a different material property. The integral equation was solved by the method of moments (MoM).

Based on our previous positive experience with differential feeding of the antenna summarized in [10] we decided to implement the same feeding scheme in our new design. As shown in Fig. 1(b), the antenna is differentially driven via two wires between the antenna flairs and generator. The source, which is used to excite the antenna, is generally specified as a complex voltage. By use of the PW card in FEKO the mismatch between

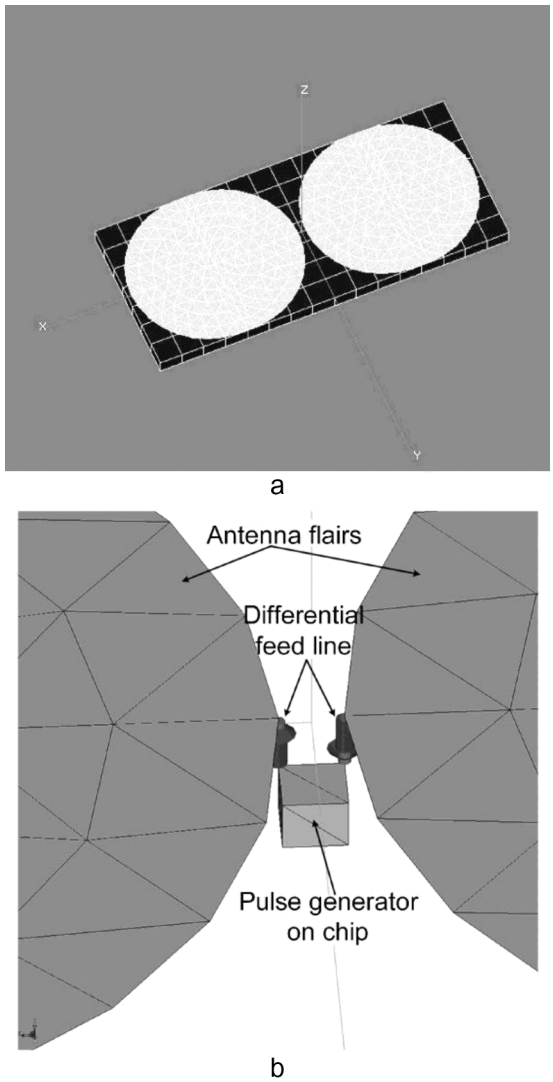

Fig. 1. Geometry of the butterfly antenna: (a) antenna on the finite substrate and (b) antenna's differential feeding.

the antenna's input impedance $\mathrm{Z_a}$ and the internal impedance of a voltage source $\mathrm{Z_g}$ is taken into account (see Fig. 2). As the antenna is differentially fed, all parameters prescribed by the PW card must be divided between the two feeding sources. In such a case, the simulation outputs in FEKO are individually presented for each feed source. To obtain the antenna's input impedance, we added the input impedances of both sources (which, due to symmetry of the problem, are equal). Henceforth in the paper, we shall always use this method.

In order to efficiently cover the selected bandwidth from 3 to 5 GHz, we chose the first derivative of Gaussian pulse with a duration of about 223 ps (i.e., at the level of 10% of the amplitude). It is well-known that by feeding of a small dipole antenna with the first derivative of the Gaussian pulse it is not possible to satisfy FCC spectral masks for indoor/outdoor unlicensed communication. Nevertheless we chose the Gaussian monocycle due to its intrinsic time frequency resolution product, which is important for such applications as positioning. Design of a waveform to satisfy FCC (or any other) spectral mask is beyond the scope of this paper.

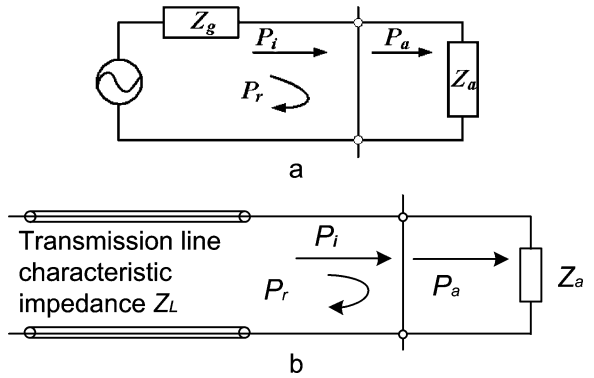

Fig. 2. Circuit models for antenna feeding (a) with and (b) without matching to generator.

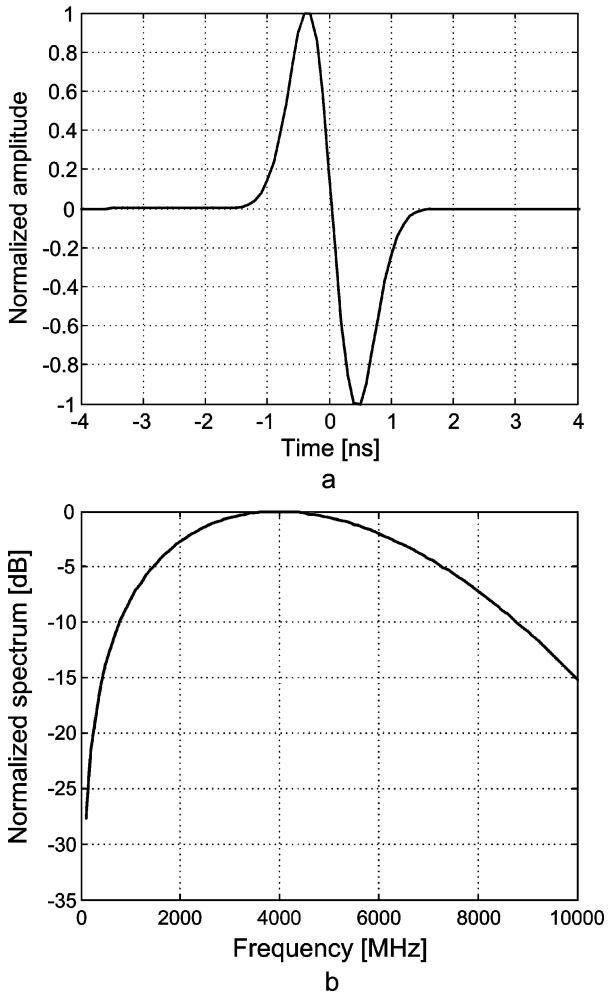

Fig. 3. Output of the pulse generator: (a) waveform and (b) frequency spectrum.

This pulse roughly covers the frequency band from 1.9 GHz to 6.5 GHz at the -3 dB level. The waveform and the pulse spectrum are shown in Fig. 3.

To calculate radiated signals in time domain, we simulated the structure in the frequency domain from 0.1 to 11 GHz. The lowest frequency is determined by the duration of the desired observation time window while the highest frequency is determined by the highest frequency of the feeding pulse spectrum at -20 dB level. To improve the time-domain resolution, zero padding must be applied up to 50 GHz. Together with the proper frequency window and the inverse Fourier transform (IFT) for calculating the radiated field in the time domain, this approach allows to analyze antenna radiation fast and accurately in the time domain. Despite of electromagnetic simulations in the frequency domain up to 11 GHz, we present frequency domain data only up to 10 GHz as this bandwidth is of major interest for us.

By choosing the differential feeding of the antenna and the feeding pulse, the first step of the co-design procedure has been carried out.

III. Electromagnetic Design of the "Antenna Plus Generator" System

In this section we optimize the antenna shape and its dimensions in free space, select the substrate material and investigate its overall influence, and optimize the position the generator with respect to the antenna flairs to obtain optimum performance. In Sections III-A and III-B, the model does not take into account the generator, and the antenna is assumed to be driven by a single wire placed between the flairs and with an internal impedance of 100 Ohm [see Fig. 2(b)]. Total source power was assumed to be fed by a transmission line with a characteristic impedance $\mathrm{Z_L}$. A mismatch between the characteristic impedance and the antenna input impedance $\mathrm{Z_a}$ would result in a part of the incident power (i.e. $\mathrm{P_i}$) being reflected back to the source as $\mathrm{P_r}$.

A. Antenna Dimensions and Shape

An antenna with a single flair of $20\times22\ \mathrm{mm}^2$ is derived upon optimizing the antenna shape and dimensions [9]. The input impedance of this antenna for different width of the feeding gap is shown in Fig. 4.

The feeding gap (slot between the antenna flairs) directly influences the antenna's input impedance and its reflection coefficient. As illustrated in Fig. 5, the shorter the spacing, the lower the reflection coefficient. These results are essential for the positioning of the RF device on the PCB and are further investigated in Section III-C.

B. Influence of the Dielectric Substrate on Antenna Performance

As the antenna is milled on a dielectric substrate, we investigated the influence of the size and dielectric permittivity of this material in this section. Two substrate dimensions were chosen: $20\times45\ \mathrm{mm}^2$ (1X) and $30\times67\ \mathrm{mm}^2$ (1.5X) with substrate thicknesses of 0.8/1.6/2/3.2 mm with a dielectric permittivity of 2.3/3.5. These thicknesses and dielectric permittivity values correspond to parameters associated with different Duroid and Rogers substrates. According to numerical simulations the substrate causes the reflection coefficient to decrease at frequencies below 5 GHz and increases it at frequencies above 6 GHz. The substrate has a significant impact on the antenna gain in terms of its maximum value and bandwidth [see Fig. 6(a)]. The highest gain is that of a structure in free space. Under certain circumstances, the dielectric substrate may decrease the antenna gain

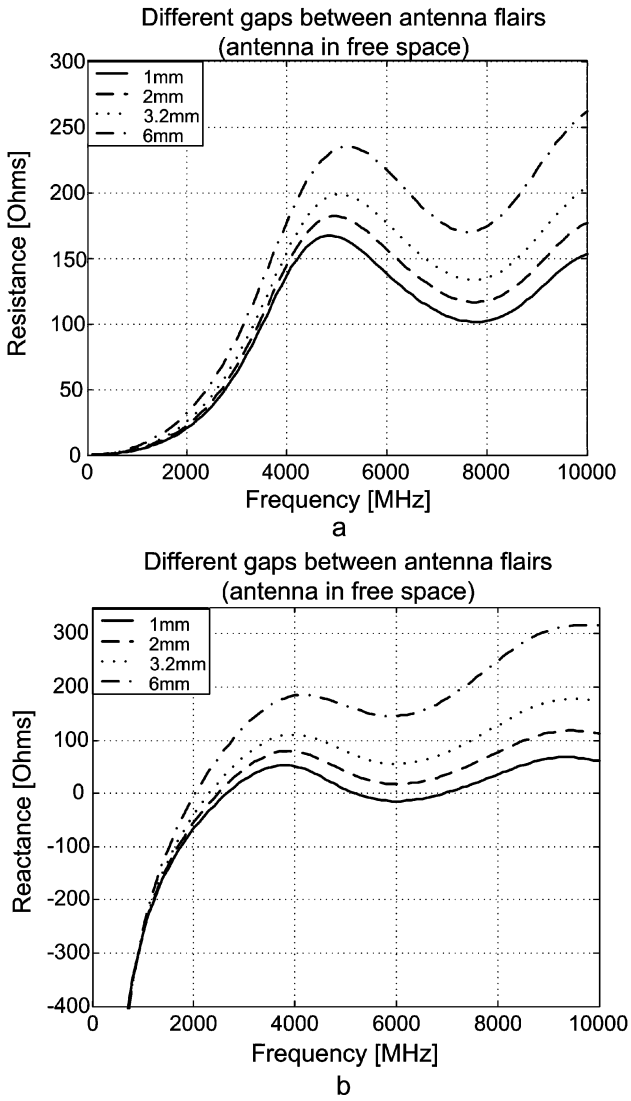

Fig. 4. Input impedance of the butterfly antenna (flair dimension of $20 \times 22\ \mathrm{mm}^2$) in free space for different widths of the feeding gap: (a) antenna resistance and (b) antenna reactance.

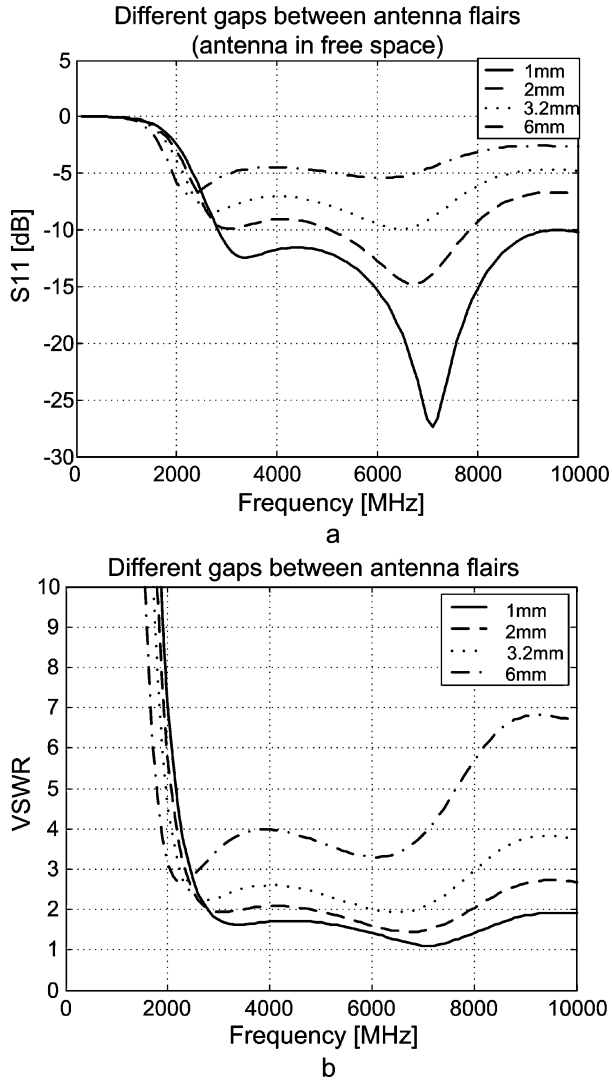

Fig. 5. (a) Antenna reflection coefficient and (b) VSWR as a function of the slot size between antenna flairs.

up to 2 dB (the direction of maximum gain is along the negative direction of Z-axis [see Fig. 1(a)], through the substrate, which in spherical coordinates corresponds to $\theta = 180$). The smaller the substrate, the higher the maximum achievable gain. The curve for the substrate 1X is close to that for free space, and the curve for the substrate 1.5X is almost equal to that for an infinite substrate.

Besides the gain, the substrate also reduces the antenna bandwidth. In comparison to free space, an infinite substrate decreases the bandwidth (-3 dB level) with about 1 GHz. The smaller the substrate, the larger the bandwidth. Increasing the substrate thickness affects both the antenna gain and the bandwidth [see Fig. 6(b)]. An increase in a substrate's dielectric permittivity has the same impact as an increase in its size.

The substrate also has some effect on the antenna radiation patterns in E-plane as can be seen in Fig. 7. The polar angle θ is counted from a positive direction of Z-axis [see Fig. 1(a)]. The antenna on the finite substrate has larger radiations upwards and along the substrate than the antenna on the infinite substrate.

Based on the simulations we chose a PCB substrate dimensions $24 \times 47\ \mathrm{mm}^2$ (1X) with a thickness of 0.8 mm and dielectric permittivity of 2.3.

C. Antenna Feeding

Next step of the co-design procedure is the optimization of the RF device (i.e., pulse generator) position with respect to the antenna. This stage consists of determining the influence of the actual device and the feeding lines on the antenna performance. The antenna is fed by two sources on both side of the RF chip.

Three possible scenarios for RF device integration were investigated (see Fig. 8):

Case 1) RF device is positioned between the antenna flairs;
Case 2) RF device is positioned aside of the antenna;
Case 3) RF device is positioned above the antenna flairs on the opposite side of the substrate.

Case 1: The microstrip feeding lines are on the same side of the substrate as the antenna flairs [see Fig. 8(a)]. The power feeding lines are orthogonal to the RF feeding lines. The distance between antenna flairs (i.e., the slot size) was 6–8 mm, mainly because of the device size, the bias/filtering circuits

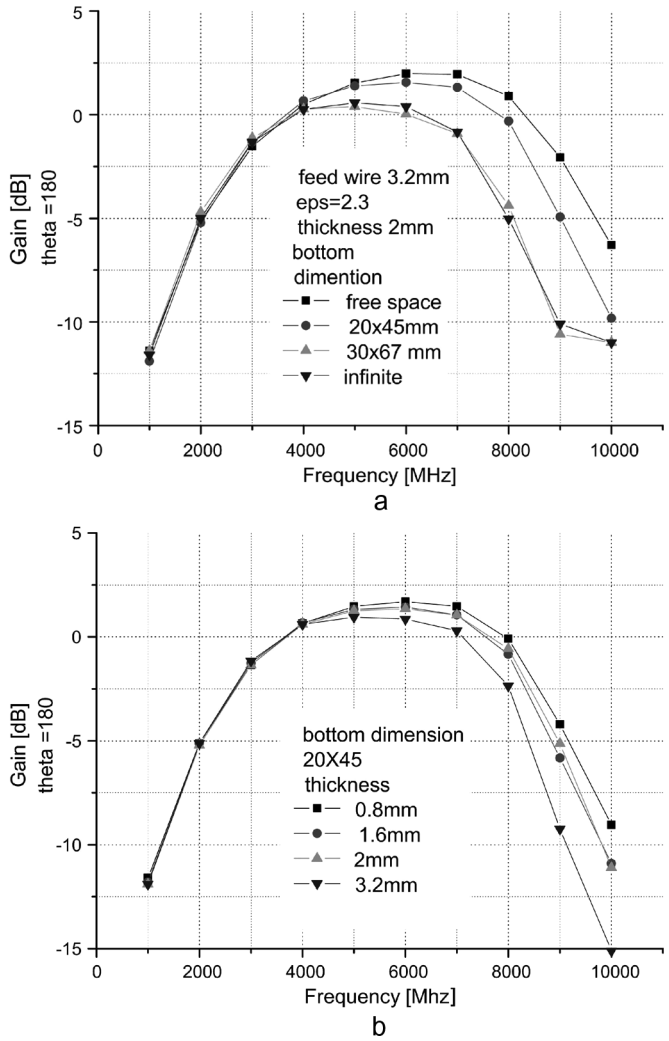

Fig. 6. (a) Antenna gain as a function of the substrate size and (b) as a function of the substrate thickness. The direction of maximum gain is through the substrate, which in spherical coordinates corresponds to $\theta = 180$.

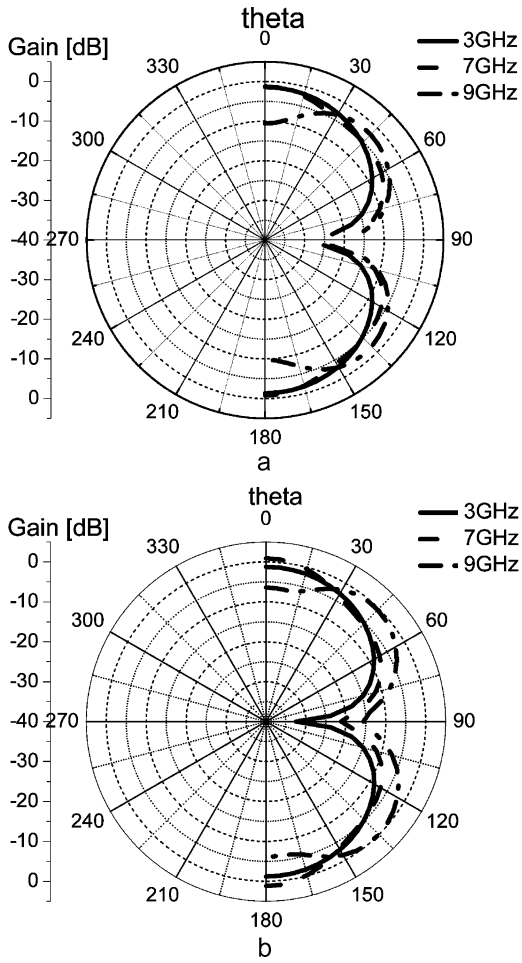

Fig. 7. Antenna radiation patterns (in dB) in E-plane for (a) infinite and (b) finite dielectric substrate.

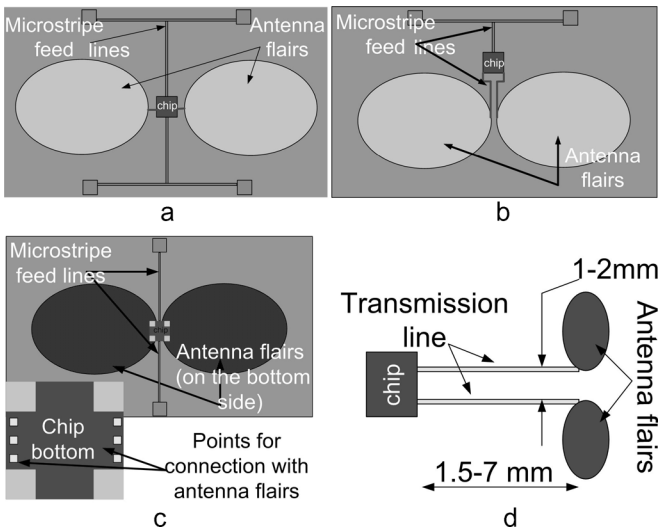

Fig. 8. Three scenarios of RF chip integration with an antenna: (a) chip is located between the antenna flairs, (b) chip is placed below the antenna flairs, (c) chip is placed on the opposite side of PCB, and (d) the feeding line in scenario 2.

around the chip, and the bond wires connecting the generator to the flairs. As mentioned in Section III-A, for optimum performance the slot size should be about 1 mm. Large slot sizes and the presence of a PEC object between the antenna flairs leads to an increase in both the antenna's input resistance and reactance. They also cause greater variations in the input impedance over the operational frequency band (see Fig. 9). As a result, the antenna cannot be matched to a generator with a real output impedance, making this scenario unfeasible.

The simulation results show that feeding lines that are in parallel to the antenna dipole moment (and thus parallel to the radiated electric field) resonate at certain frequencies and are considered as parasitic antennas. This phenomenon directly influences the antenna impedance, the reflection coefficient and changes the antenna radiation patterns (see Fig. 9).

Case 2: The antenna flairs are placed 1 mm apart [see Fig. 8(b)]. The RF device and all other biasing circuits are mounted on the same side of the dielectric substrate along with the antenna flairs. They are placed below the antenna flairs at a distance of approximately 1.5–5 mm [Fig. 8(b)]. The chip is connected to the antenna by a symmetric transmission lines formed by two metal strips [see Fig. 8(d)]. In this scenario, both the RF device and the transmission line are placed asymmetrically with respect to the feeding point of the antenna, resulting

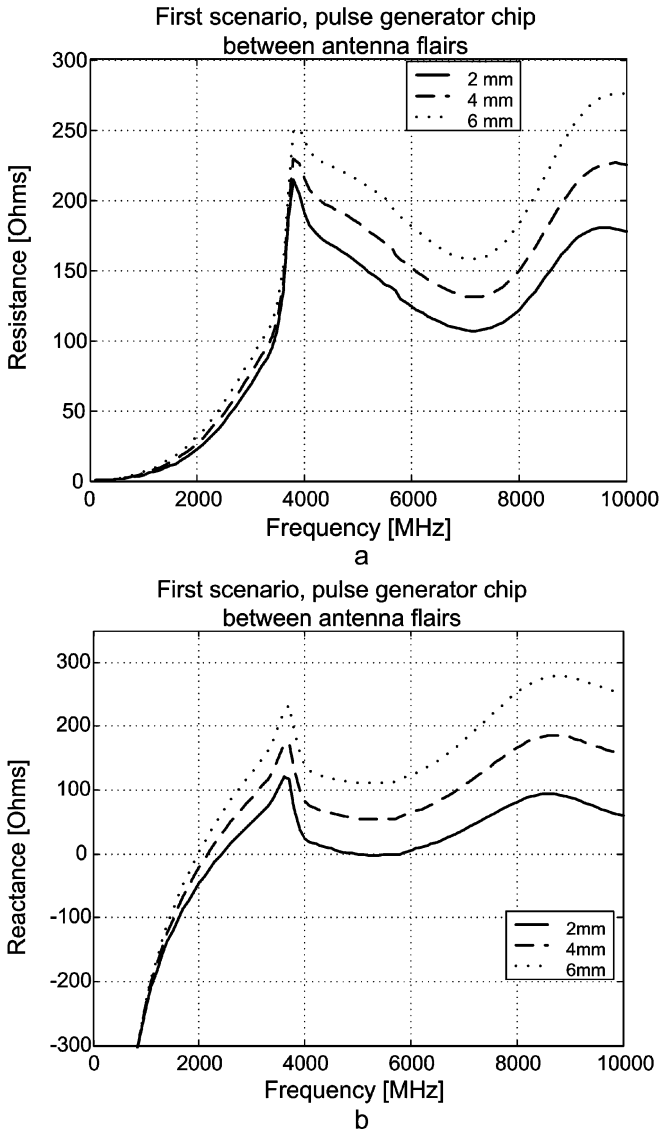

Fig. 9. Case 1: simulated antenna input impedance for the different distances between antenna flairs: (a) resistance and (b) reactance.

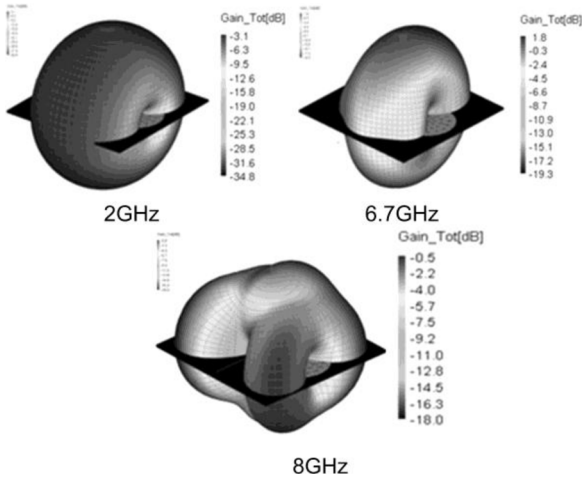

Fig. 10. Case 2: simulated antenna radiation patterns at different frequencies.

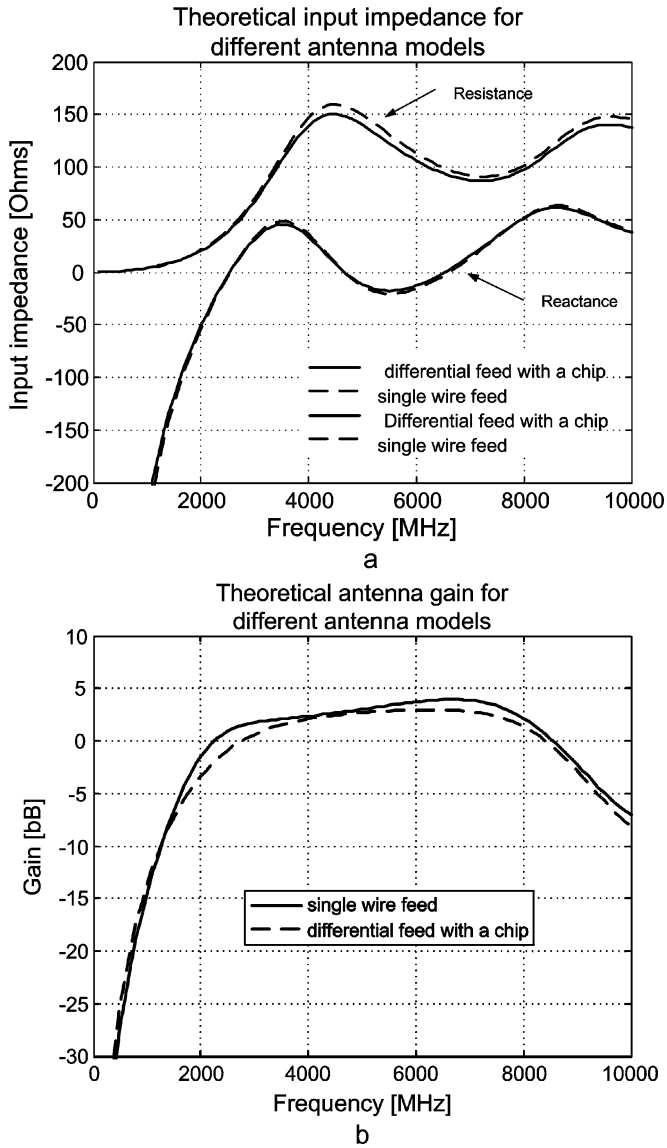

Fig. 11. Case 3: simulated input (a) impedance and (b) antenna gain.

in asymmetric radiation patterns at frequencies above 6 GHz (see Fig. 10). Presence of a transmission line reduces flexibility in the design of both the RF device and the antenna, fixing their impedance to a certain value, which is constant over a whole frequency band. Thus this scenario is not acceptable either.

Case 3: The RF device and transmission lines are placed on the lower side (i.e., directly below the spacing of the flairs) of the dielectric substrate, whereas the antenna flairs [see Fig. 8(c)] are milled on the upper side of the PCB. The spacing of the flairs is kept as small as possible (i.e., 1 mm) to obtain optimum antenna performance. Using copper vias, the generator is connected to the antenna flairs. All metal connects are perpendicular to the antenna dipole moment, which minimizes their influence on antenna characteristic. In this scenario, the antenna's input impedance is almost the same as that for the ideal case, in which the antenna is excited by a current flowing from flair to flair [see Fig. 11(a)].

Due to metallization (i.e., the RF device and transmission lines) on the lower side of the substrate, from 3–10 GHz there is a 10 Ω deviation in the input resistance of the antenna (with respect to an antenna without a chip). The imaginary part of

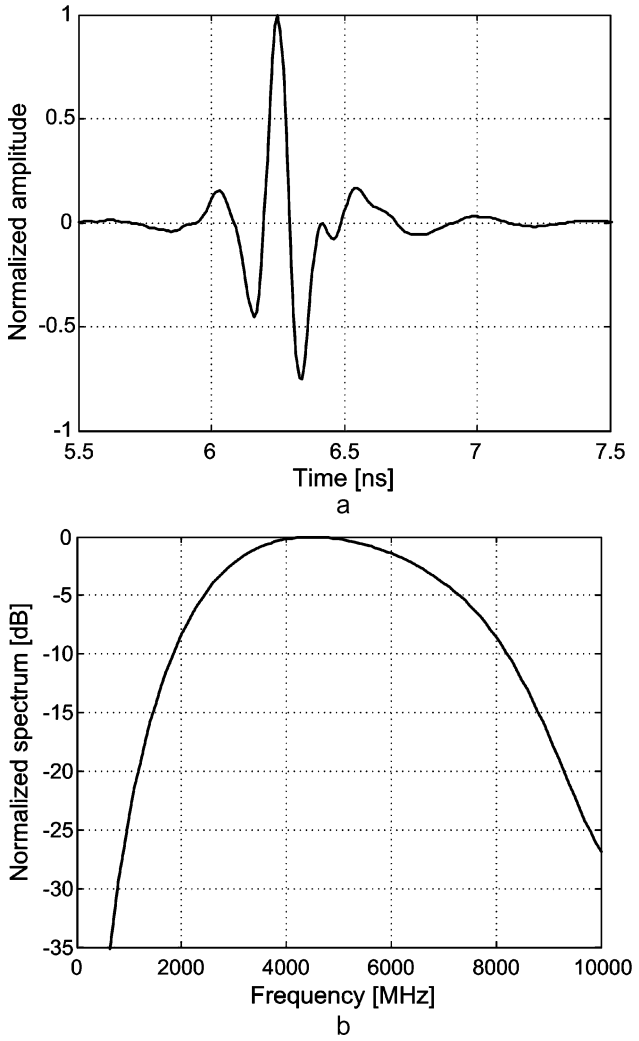

Fig. 12. Simulated antenna radiation into $\theta = 180$ direction by antenna feeding with 223 ps pulse: (a) transmitted waveform and (b) spectrum of the transmitted signal.

the antenna input impedance remains constant with and without metallization. Power feeding lines do not cause any variations in the input impedance nor in the gain of the antenna. The presence of the RF device results in small losses in the antenna gain [Fig. 11(b)] of about 1.5 dB at low frequencies (1.8–3 GHz) and 1–2 dB at higher frequencies (6–10 GHz).

Based on these simulations, we chose design 3. The antenna input resistance in the operational band varied from 90 to 150 Ω, while the reactance varied from about -15 to 60 Ω. Being differentially fed by a source with 100 Ω output impedance; the antenna operates (in terms of gain defined at -3 dB level) from 2.8 to 8.3 GHz and exhibits a gain from 0 to 3 dBi. Being fed by a 223 ps monocycle pulse as on Fig. 3(a) the antenna radiates along the negative direction of Z-axis a pulse with a waveform show in Fig. 12(a) and a bandwidth from approximately 2.8 to 6.7 GHz at -3 dB level [Fig. 12(b)]. The main pulse with the duration of about 450 ps is followed by 550 ps—long ringing.

IV. Gaussian Impulse Generator

In our previous paper [10] we investigated a generator with differential outputs that are fed to the antenna via a double semi-rigid cable, resulting in an improved match of the generator and the antenna, an improved magnitude response and reduced ringing of the radiated pulse.

In the generator, pulse position modulation (PPM) is used to encode the binary transmitted data. The impulse generator consists of a cascade of a fast triangular pulse generator and a Gaussian filter (i.e., a filter with a Gaussian impulse response). The filter is implemented as a cascade of three complex first-order systems (CFOS), which, in turn, consist of gm-C sections that employ differential pairs with partial positive feedback to improve the bandwidth. The entire transmitter consists of the modulator with the impulse generator and the antenna (see Fig. 13).

Voltage buffers, such as source followers are generally employed to drive a resistive load [see Fig. 13(a)]. The super-source follower is used in MOS technologies to reduce its output resistance. This circuit employs negative feedback through M2 to reduce the output resistance. Two "super source followers" are used to buffer the differential outputs of the Gaussian pulse generator to the input of the antennas [12].

The voltage buffers allow compensation of a variable load impedance and matching to the antenna [see Fig. 14]. The buffers have been adjusted to the input impedance of the antenna at frequency of 6.5 GHz. At this frequency, a 100 Ω differential output impedance is required.

V. Experimental Verification

The complete pulse generator is fabricated in IBM 0.18 μm Bi-CMOS IC technology. Measurements show the correct operation of the circuit for supply voltages of 1.8 V and a power consumption of 45 mW. When wire bonding is taken into account, the measured output pulse is longer in duration than the simulated one. The measured pulse can be reasonably well approximated by the Gaussian first derivative with a pulse duration of about 470 ps at 10% of amplitude level (see Fig. 15). Discrepancy between measured and approximating signal in frequency domain below -10 dB level is not important for time domain results.

We have investigated possible causes of the widening of the output pulse. A square waveform (i.e., the clock signal), when applied to the input of the transmitter is eventually transformed into a triangular waveform used to trigger the impulse response of the Gaussian filter. The latter may have a much longer rise/fall time. However, this has minimal effect on the pulse width of the Gaussian waveform. At transistor level, due to channel length modulation, the current delivered to the CFOS stages (i.e., in the Gaussian pulse generator) could be lower than expected and thus the deviance in the frequency response. As a result, the pulse width of the measured Gaussian waveform fed to the antenna is larger than that simulated. Finally, off-chip parasitic (e.g., bond wire inductances and capacitances) or even technological imperfections during fabrication could also have attributed to this.

In order to experimentally validate the integration and co-design concepts with the manufactured generator, we scaled-up the antenna geometry (proportionally to the ratio between the duration of measured and simulated pulse from the generator).

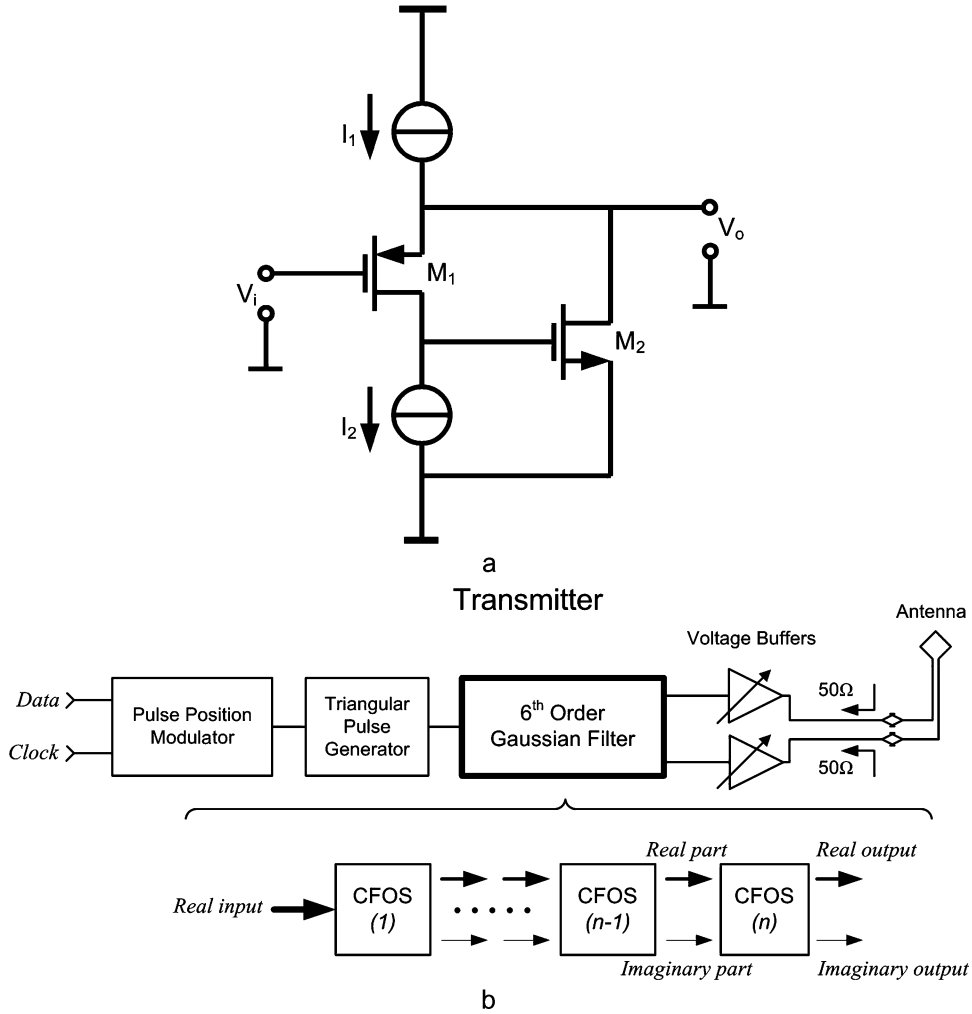

Fig. 13. (a) Super source follower and (b) block diagram of an integrated impulse generator.

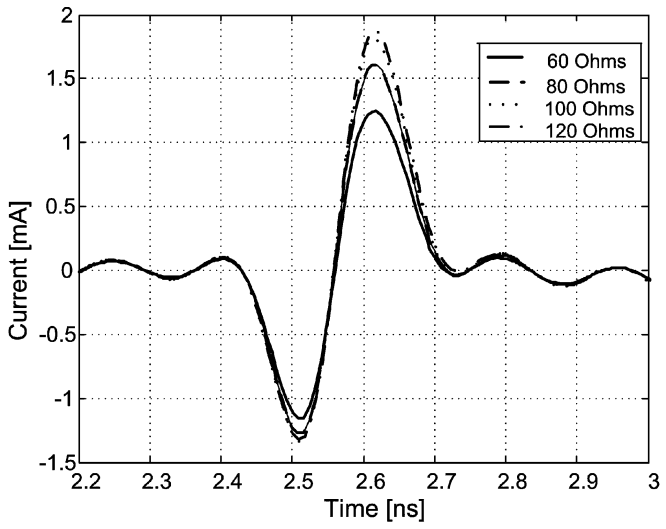

Fig. 14. Simulated output current from the voltage buffer for different impedances of the load.

The antenna flairs were milled on the same PCB with the RF device and bias circuits (see Fig. 16).

The pulse generator is triggered by a 10 MHz function generator. To measure the radiated waveforms we used a dielectric wedge antenna (DWA) [13] as the receive antenna. As DWA has a flat receive transfer function from 1 to 4.8 GHz, it faithfully reproduces on its output terminals waveforms of the incident electromagnetic wave with duration more than 200 ps. The radiated waveforms were measured at the distance of approximately 35 cm from the transmit antenna (see Fig. 17).

The measured waveform and the simulated prediction of the radiation from the antenna have being fed with a pulse as in Fig. 15 are shown in Fig. 18. Late-time ringing in the measured data is caused by the low-frequency cut-off of the receive antenna. Furthermore, in the simulated data we observed a pre-pulse at 4.7 ns, which is absent in the measured data. The reason for the pre-pulse is scattering from a PEC body representing the RF device. In reality the chip has a more complicated structure and does not produce such a pre-pulse. For the rest a good agreement between measured data and the theoretical prediction of the developed model of the system "antenna plus generator" is observed. We see that the theoretical model of the "antenna plus generator" system developed precisely describes the real antenna performance.

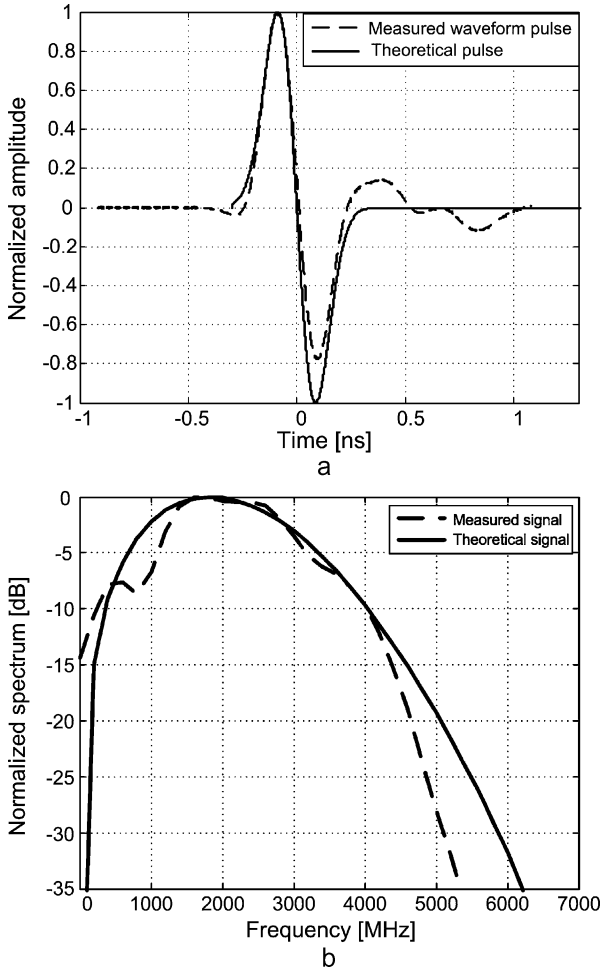

Fig. 15. Measured output waveform from the pulse generator and its approximation with the first derivative of Gaussian pulse: (a) time domain and (b) frequency domain.

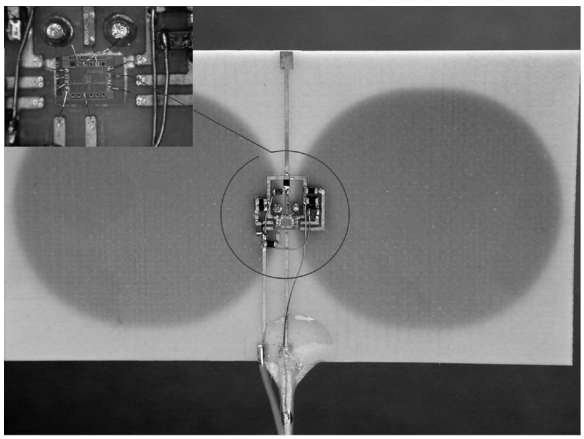

Fig. 16. Integrated chip on the back side of the antenna.

VI. Discussion and Conclusions

This paper describes integration of a pulse generator into an UWB antenna. Both parts of the system are co-designed, i.e., matched in terms of impedance and the generator's influence on the antenna's radiation properties is taken in to account. The resulting design does not require intermediate transmission lines

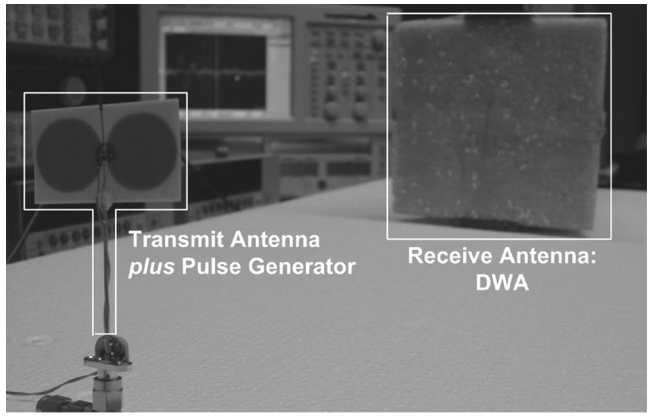

Fig. 17. Measurement setup: (left) butterfly antenna with the integrated impulse generator and (right) dielectric wedge antenna.

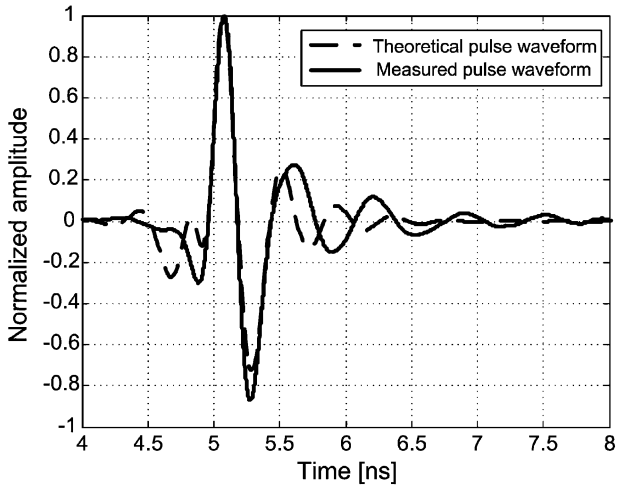

Fig. 18. Transmitted waveforms: measured and simulated by antenna feeding with 470 ps pulse.

conventionally placed between generator and antenna, thus offering extra flexibility in matching between RF device and antenna. Furthermore, the design also prevents excitation of the common mode current.

The co-design is a three-step approach: first, the interface between the RF device and the antenna is identified (i.e., differential feeding) and the waveform of the signal to be radiated is identified; this is a Gaussian monocycle with a pulse width of 223 ps. Second, an electromagnetic design of the complete system including the generator, antenna and PCB is performed, resulting in the requested antenna geometry (i.e., size and shape of the antenna flairs and size, thickness and dielectric permittivity of the substrate), the position of the RF device with respect to the antenna flairs and the input impedance of the antenna. Finally, the output circuits of the generator (i.e., voltage buffers) are designed to match the generator directly to the antenna input impedance. As a result of this procedure, we designed an integrated system, which transmits a 450 ps pulse with approximately 550 ps ringing covering a (-3 dB) bandwidth from approximately 2.8 to 6.7 GHz. This is a frequency range wider than originally aimed for.

The co-design and integration were experimentally verified by placing the antenna flairs, the generator and all other biasing/filtering circuits on a single PCB. The generator used for verification fires an excellent approximation of the Gaussian monocycle, however due to technical limitations in the chip design the pulse duration differs from one used for original antenna design. To accommodate the output signal of the manufactured generator scaled-up the antenna and integrated the generator in this antenna version. The measured transmitted waveforms matched well those predicted by the theoretical model.

By integrating the butterfly antenna with a generator an intermediate transmission line has been eliminated and the total volume of the front-end has been decreased. Furthermore, in comparison with [10] the magnitude response was improved and ringing of the radiated pulse reduced by direct matching of the generator to the antenna. In addition this design can easily be realized.

In further research the generator will be redesigned in order to produce a required 223 ps long pulse. With such a generator, the "antenna plus generator" system will operate within a specified frequency band from approximately 3 GHz to 8 GHz.

ACKNOWLEDGMENT

The authors would like to thank W. Straver for his invaluable help in mounting the pulse generator with the antenna, as well as J. Zijderveld and P. Hakkaart for their outstanding technical support.

REFERENCES

[1] FCC 02-48—Federal Communication Commission, "First Report and Order Regarding Ultra Wideband Transmission System," [Online]. Available: http://www.fcc.gov adopted: Feb. 14, 2002, released: Apr. 22, 2002

[2] H. Schantz, "A brief history of ultra wideband antennas," *IEEE Aerosp. Electromagn. Syst. Mag.*, vol. 19, no. 4, pp. 22–26, Apr. 2004.

[3] M. Klemm and G. Troster, "Integration of electrically small UWB antennas for body-worn sensor applications," *Wideband Multi-band Antennas Arrays*, pp. 141–146, 2005.

[4] S. Bories, H. Ghannoum, and C. Roblin, "Robust planar stripline monopole for UWB terminal applications," in *Proc. IEEE Int. Conf. UWB*, Sep. 2005, pp. 80–84.

[5] H. G. Schantz, "Planar elliptical element UWB dipole antennas," in *Proc. IEEE Antennas and Propagation Society Int. Symp.*, 2002, vol. 3, pp. 44–47.

[6] A. Yarovoy, R. Pugliese, J. Zijderveld, and L. Ligthart, "Antenna development for UWB impulse radio," in *Proc. 34th Eur. Microwave Conf.*, 2004, pp. 1257–1260.

[7] N. Agrawall, G. Kumar, and K. P. Ray, "Wide-band planar monopole antennas," *IEEE Trans. Antennas Propag.*, vol. 46, no. 2, pp. 294–295, Feb. 1998.

[8] H. Schantz, "Bottom fed planar elliptical UWB antennas," in *Proc. IEEE Conf. Ultra-Wideband Systems and Technologies*, Nov. 2003, pp. 219–223.

[9] A. Vorobyov, J. Zijderfeld, A. Yarovoy, and L. Ligthart, "Impact of common mode currents on miniaturized UWB antenna performance," *Eur. Microw. Week*, pp. 285–289, Oct. 2005.

[10] S. Bagga, A. V. Vorobyov, S. A. P. Haddad, A. G. Yarovoy, W. A. Serdijn, and J. R. Long, "Co-design of an impulse generator and miniaturized antennas for IR-UWB," *IEEE Trans. Microw. Theory Tech., Special Issue on UWB*, vol. 54, no. 4, pt. 2, pp. 1656–1666, Apr. 2006.

[11] *"FEKO Manual"* [Online]. Available: http://www.feko.info

[12] P. Gray, P. Hurst, S. Lewis, and R. Meyer, *Analysis and Design of Analog Integrated Circuits*, 4th ed. New York: Wiley, 2001.

[13] A. Yarovoy, A. Schukin, I. Kaploun, and L. Ligthart, "The dielectric wedge antenna," *IEEE Trans. Antennas Propag.*, vol. 50, no. 10, pp. 1460–1472, Oct. 2002.

Alexander V. Vorobyov (M'06) received the M.S. degree in radiophysics and electronics from Kharkov State University, Ukraine, in 2000. He is currently working toward the Ph.D. degree at Delft University of Technology, Delft, The Netherlands.

In 2002–2003, he was with the Department of Applied Mechanics, Kharkov Academy of Fire Safety, as an Assistant Lecturer where he also worked on remote sensing of natural raw materials with respect to centers of self-warming up. In 2004, he joined the International Research Centre for Telecommunications-Transmission and Radar, Delft University of Technology. His main research interests are in applied electromagnetics, in particular in design, miniaturization and optimization of UWB antennas for telecommunications.

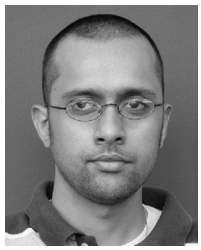

Sumit Bagga (M'04) was born in New Delhi, India, in 1977. He received the B.S. degree (with distinction) from Shivaji University, Kolhapur, India and the M.Eng. degree from the University of Brasilia (UnB), Brazil, in 1999 and 2002, respectively, both in electrical engineering.

In November 2002, he joined the Electronics Research Laboratory (ELCA-EEMCS), Delft University of Technology, Delft, The Netherlands, where he is involved with designing transceiver architectures and circuits for ultrawideband (UWB) communications in the Ad-hoc Impulse Radio: Local Instantaneous Networks (AIR-LINK) project under the FREEBAND initiative. His research interests include high-speed, low-power analog integrated circuits for RF and UWB wireless communications.

Mr. Bagga received the Best Paper Award from UWBST and IWUWBS 2004.

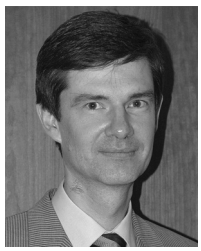

Alexander G. Yarovoy (M'96–SM'04) graduated with the Diploma (with honors) in radiophysics and electronics and received the Cand. Phys. Math. Sci. and Dr. Phys. Math. Sci. degrees in radiophysics all from Kharkov State University, Ukraine, in 1984, 1987, and 1994, respectively.

In 1987, he joined the Department of Radiophysics, Kharkov State University, as a Researcher and became a Professor in 1997. From September 1994 through 1996, he was with the Technical University of Ilmenau, Germany, as a Visiting Researcher. Since 1999, he is with the International Research Centre for Telecommunications-Transmission and Radar (IRCTR), Delft University of Technology, The Netherlands, where he coordinates all UWB-related projects. His main research interests are in ultrawideband (UWB) technology and its applications (in particular, UWB radars) and applied electromagnetics (in particular, UWB antennas).

Prof. Yarovoy is the recipient of a 1996 International Union of Radio Science (URSI) "Young Scientists Award" and a co-recipient of the European Microwave Week Radar Award in 2001 for the Paper that Best Advances the State-of-the-Art in Radar Technology. He served as the Co-Chairman and the Technical Program Committee Chair of the Tenth Int. Conf. on Ground Penetrating Radar (GPR2004), Delft, and the Secretary of the 1st European Radar Conference (EuRAD'04), Amsterdam, The Netherlands.

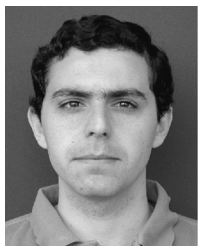

Sandro A. P. Haddad (M'02) was born in Annapolis, Brazil, in 1977. He received the B.Eng. degree from the University of Brasilia (UnB), Brasilia, Brazil, in 2000, with honors. He is working toward the Ph.D. degree at Delft University of Technology, Delft, The Netherlands, since 2001.

His research is a part of the Biomedical Signal Processing Platform for Low-Power Real-Time Sensing of Cardiac Signals (BioSens). His research interests include low-voltage, ultralow power analog electronics and biomedical systems, and high frequency analog integrated circuits for ultrawideband communications.

Wouter A. Serdijn (M'98) was born in Zoetermeer ("Sweet Lake City"), The Netherlands, in 1966. He received the 'ingenieurs' (M.Sc.) and Ph.D. degrees from Delft University of Technology, Delft, The Netherlands, in 1989 and 1994, respectively.

In 1984, he joined the Electronics Research Laboratory, Delft University of Technology. Since 2002, he is a Work Package Leader in the Freeband Impulse project AIR-LINK, aiming at high-quality, wireless short-distance communication, employing UWB radio. He teaches analog electronics, micropower analog IC design and electronic design techniques. He is the coeditor and coauthor of the books *Research Perspectives on Dynamic Translinear and Log-Domain Circuits* (Kluwer Academic Publishers, Boston, 2000), *Low-Voltage Low-Power Analog Integrated Circuits* (Kluwer Academic Publishers, Boston, 1995) and *Dynamic Translinear and Log-Domain Circuits* (Kluwer Academic Publishers, Boston, 1998). He authored and coauthored more than 150 publications and presentations. His research interests include low-voltage, ultra low-power, high-frequency and dynamic-translinear analog integrated circuits along with circuits for RF and UWB wireless communications, hearing instruments and pacemakers.

Dr. Serdijn received the EE Best Teacher Award in 2001 and 2004. He has served as an Associate Editor for the IEEE TRANSACTIONS ON CIRCUITS AND SYSTEMS—I and the IEEE TRANSACTIONS ON CIRCUITS AND SYSTEMS—II. He was tutorial session Co-Chair for ISCAS'2003, Analog Signal Processing Track Co-Chair for ISCAS'2004, Chair of the Analog Signal Processing Technical Chapter of the IEEE CAS society, Analog Signal Processing Track Co-Chair for ICECS'2004, Technical Program Committee member for the 2004 International Workshop on Biomedical Circuits and Systems, as Analog Signal Processing Track Co-Chair for ISCAS'2005, and International Program Committee member for IASTED CDD'2005, and currently (again) serves as an Associate Editor for the IEEE TRANSACTIONS ON CIRCUITS AND SYSTEMS—I and as a member of the Board of Governors of the Circuits and Systems Society.

John R. Long (M'93) received the B.Sc. degree in electrical engineering from the University of Calgary, Calgary, ON, Canada, in 1984, and the M.Eng. and Ph.D. degrees in electronics from Carleton University, Ottawa, ON, Canada, in 1992 and 1996, respectively.

He was employed for ten years by Bell-Northern Research, Ottawa (now Nortel) involved in the design of ASICs for Gbit/s fibre-optic transmission systems, and for five years as an Assistant and then Associate Professor at the University of Toronto. He joined the faculty at the Delft University of Technology, Delft, The Netherlands, in January 2002 as Chair of the Electronics Research Laboratory. His current research interests include: low-power transceiver circuitry for highly-integrated wireless applications, and electronics design for high-speed data communications systems.

Prof. Long currently serves on the Program Committees of the International Solid-State Circuits Conference (ISSCC), the European Solid-State Circuits Conference (ESSCIRC), the IEEE Bipolar/BiCMOS Circuits and Technology Meeting (BCTM), and the European Microwave Conference. He is a former Associate Editor of the IEEE JOURNAL OF SOLID-STATE CIRCUITS. He received the NSERC Doctoral Prize and Douglas R. Colton and Governor General's Medals for research excellence, and Best Paper Awards from ISSCC 2000 and IEEE-BCTM 2003.

Zoubir Irahhauten (M'03) received the M.Sc.E.E. degree from Delft University of Technology, Delft, The Netherlands, in 2002, where he is currently working toward the Ph.D. degree.

His areas of interest include propagation modeling of UWB wireless channels and positioning.

Leo P. Ligthart (F'02) was born in Rotterdam, The Netherlands, on September 15, 1946. He received the Engineer's degree (*cum laude*) and the Doctor of Technology degree from Delft University of Technology, Delft, The Netherlands, in 1969 and 1985, respectively, and the Doctorates (honoris causa) degree from Moscow State Technical University of Civil Aviation, Moscow, Russia, in 1999, and the Doctorates (honoris causa) degree from Tomsk State University of Control Systems and Radioelectronics, Tomsk, Russia, in 2001.

Since 1992, he has held the Chair of Microwave Transmission, Radar and Remote Sensing in the Department of Information Technology and Systems, Delft University of Technology. In 1994, he became Director of the International Research Center for Telecommunications-Transmission and Radar. His principal areas of specialization include antennas and propagation, radar and remote sensing, but he has also been active in satellite, mobile, and radio communications.